Tree-penguin interference and tests for $\cos\gamma<0$ in rare $B\to PP$, PV, and VV decays

Wei-Shu Hou

Department of Physics, National Taiwan University, Taipei, Taiwan 10764, Republic of China

Kwei-Chou Yang

Institute of Physics, Academia Sinica, Taipei, Taiwan 11529, Republic of China
and Department of Physics, Chung Yuan Christian University, Chung-li, Taiwan 32023, Republic of China

Recent rare $B\to PP$, PV decay data suggest that factorization holds well if, contrary to current fits, one has $\cos\gamma<0$ where $\gamma\equiv\arg(V_{ub}^*)$. We update previous results with light cone sum rule form factors, which seem to work better. We then discuss various $B\to VV$ modes as well as the $K^*\eta$ modes. Finding the pattern of $\rho^+\omega^0<\rho^+\rho^0$, $K^{*+}\rho^{-,0}>K^{*0}\rho^+$, $K^{*+}\omega^0>K^{*0}\omega^0$ and $K^{*+}\eta>K^{*0}\eta$ would strengthen the support for $\cos\gamma<0$. The electroweak penguin amplitude enhances (suppresses) the $K^{*+}\rho^0$ ($K^{*0}\rho^0$) rate by a factor of 2, and finding $K^{*+}\rho^0\simeq K^{*+}\rho^-$ would be strong evidence for the electroweak penguin amplitude.

PACS number(s): 12.15.Hh, 12.15.Mm, 13.25.Hw

I. INTRODUCTION

Experimentally, a number of hadronic rare B decay modes have been observed [1–3] in the last two years. They may allow us access [4–7] to unitarity angles of the Kobayashi-Maskawa (KM) matrix such as γ [$\equiv\arg(V_{ub}^*)$ in standard phase convention], by exploiting interference between tree and penguin amplitudes in these modes. The presently observed decay processes can be catalogued into two classes. The first class, e.g., $B\to\rho\pi$, is dominated by tree (T) level $b\to u$ transitions, but may have sizable penguin (P) contributions. The second class, e.g., $B\to K\eta'$, $K\pi$, and the newly observed $K^{*+}\pi^-$ mode, are penguin dominant processes which may have sizable T/P.

Two-body decays of B mesons are usually studied under the factorization hypothesis. Based on this hypothesis, the decay amplitude is given in terms of a weak transition amplitude and the decay constant of a factorized final state meson. Nonfactorizable contributions are lumped into the effective number of colors N_{eff} which may deviate from $N_c=3$. The current fits of KM parameters give γ in the range of $60°-70°$ [8], which heavily relies on the lower limit $\Delta m_{B_s}>12.4\text{ ps}^{-1}$ from combining CERN e^+e^- Collider LEP, Collidier Detector at Fermilab (CDF) and SLAC Large Detector (SLD) data. With a little loosened limit $\Delta m_{B_s}>10.2\text{ ps}^{-1}$ [9] at 95% C.L., some room is allowed for negative $\cos\gamma$. If one adopts, however, the currently favored $\gamma\simeq 60°-70°$, it is difficult to explain present data such as $K^+\pi^-\sim K^0\pi^+\sim K^+\pi^0\sim 1.5\times10^{-5}$, $\pi^+\pi^-<0.84\times10^{-5}$, and the strength of the newly observed $\rho^0\pi^+\sim 1.5\times10^{-5}$ and $K^{*+}\pi^-\sim 2.2\times10^{-5}$ [3]. All the data so far therefore seem to prefer $\cos\gamma<0$ if factorization holds [7], except the size of $K^+\omega^0\sim 1.5\times10^{-5}$ [2] which cannot be explained by factorization [see Note added]. However, all modes with branching ratios (Br) of order 10^{-5} or more will likely be updated or measured soon by CLEO and the B factories. It is thus of interest to explore any additional modes that can shed further light on γ. In this paper we extend Ref. [7] and study

additional channels [10] for which the γ range can be probed.

We update the $B\to PP$ and PV modes (P, V stand for pseudoscalar and vector mesons) with form factors from light-cone (LC) sum rules [11], which seem to give a better fit to data than using Bauer-Stech-Wirbel (BSW) form factors [12]. We find further that some VV modes and the $K^*\eta$ modes are promising. Processes that are basically pure T (e.g. $\rho^+\rho^0$) or pure P (e.g. $K^{(*)}\phi$) depend only weakly on γ, and thus offer direct tests of factorization. If large CP asymmetries (a_{CP}) are observed in the $K^{(*)}\phi$ modes, it could be a signal for new physics. The paper is organized as follows. In Sec. II a brief review of the theoretical framework is given. We then sketch how sensitivity to γ angle emerges. In Sec. III we discuss in detail the hints of negative $\cos\gamma$ from existing data. We show that the form factors from LC sum rules are preferred by data. Adopting LC sum rule form factors, in Sec. IV we study the VV modes as well as some other modes that can offer further tests for $\cos\gamma<0$ or the factorization hypothesis. Finally, the discussion and conclusion are presented in Sec. V.

II. THEORETICAL FRAMEWORK

The standard starting point is the effective $\Delta B=1$ weak Hamiltonian

$$\mathcal{H}_{\text{eff}}=\frac{G_F}{\sqrt{2}}\left\{V_{uq}^*V_{ub}[c_1(\mu)O_1^u(\mu)+c_2(\mu)O_2^u(\mu)]\right.$$
$$+V_{cq}^*V_{cb}[c_1(\mu)O_1^c(\mu)+c_2(\mu)O_2^c(\mu)]$$
$$\left.-V_{tq}^*V_{tb}\sum_{i=3}^{10}c_i(\mu)O_i(\mu)\right\}+\text{H.c.},\qquad(2.1)$$

where $q=d,s$, and

$$O_1^u=(\bar{q}u)_{V-A}(\bar{u}b)_{V-A},\qquad O_2^u=(\bar{q}_\beta u_\alpha)_{V-A}(\bar{u}_\alpha b_\beta)_{V-A},$$
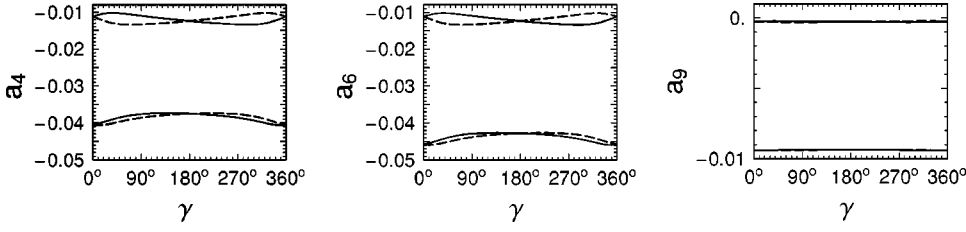
FIG. 1. Penguin coefficients a_4, a_6 and a_9 vs γ, where the solid (dashed) curves are for $b \rightarrow d\bar{q}q$ ($\bar{b} \rightarrow \bar{d}\bar{q}q$) and the upper (lower) curves correspond to $\mathrm{Re}(a_i)[\mathrm{Im}(a_i)]$.

$$O_1^c = (\bar{q}c)_{V-A}(\bar{c}b)_{V-A}, \qquad O_2^c = (\bar{q}_\beta c_\alpha)_{V-A}(\bar{c}_\alpha b_\beta)_{V-A},$$
$$(2.2)$$

$$O_{3(5)} = \sum_{q'} (\bar{q}'q')_{V-A(V+A)}(\bar{q}b)_{V-A},$$

$$O_{4(6)} = \sum_{q'} (\bar{q}'_\beta q'_\alpha)_{V-A(V+A)}(\bar{q}_\alpha b_\beta)_{V-A},$$

$$O_{7(9)} = \frac{3}{2} \sum_{q'} e_{q'}(\bar{q}'q')_{V+A(V-A)}(\bar{q}b)_{V-A},$$

$$O_{8(10)} = \frac{3}{2} \sum_{q'} e_{q'}(\bar{q}'_\beta q'_\alpha)_{V+A(V-A)}(\bar{q}_\alpha b_\beta)_{V-A},$$

with O_{3-6}, O_{7-10} the QCD, electroweak penguin operators and $(\bar{q}_1 q_2)_{V\pm A} \equiv \bar{q}_1 \gamma_\mu (1 \pm \gamma_5) q_2$. The decay amplitude is computed by evaluating the hadronic matrix elements of $\mathcal{H}_{\mathrm{eff}}$, i.e.

$$c_i(\mu)\langle O_i(\mu)\rangle = c_i(\mu) g_{ij}(\mu)\langle O_j\rangle_{\mathrm{fac}} \equiv c_j^{\mathrm{eff}}\langle O_j\rangle_{\mathrm{fac}},$$
$$(2.3)$$

where the μ-dep. of $\langle O_i(\mu)\rangle$ has been taken out through the matrix $g_{ij}(\mu)$ which cancels the μ-dep. of $c_i(\mu)$ to give c_j^{eff}, which should not depend on the theoretical scale parameter μ. The matrix elements $\langle O_j\rangle_{\mathrm{fac}}$ are evaluated at the factorization scale μ_f by equating it to products of matrix elements of quark bilinears, the evaluation of which is done by form factor models. It can be shown that the c_i^{eff}s are μ, scheme and gauge independent [13], but it should be at the same scale μ_f where one evaluates $\langle O_j\rangle_{\mathrm{fac}}$. Whether, or how, factorization actually works, however, is not well understood.

The decay amplitudes derived from the factorization approach are given in terms of effective parameters a_i^{eff}, where $a_{2j}^{\mathrm{eff}} = c_{2j}^{\mathrm{eff}} + (1/N_c)c_{2j-1}^{\mathrm{eff}}$ and $a_{2j-1}^{\mathrm{eff}} = c_{2j-1}^{\mathrm{eff}} + (1/N_c)c_{2j}^{\mathrm{eff}}$ ($j = 1, \ldots, 5$). In what follows, we adopt the values of a_i^{eff} given in Ref. [14] which are evaluated at $\mu_f = m_b$, use $N_c = 3$, and ignore final state interactions (FSI). Since the presently observed modes are largely color allowed, most results

here are insensitive to $N_{\mathrm{eff}} \neq N_c$. The influence of $N_{\mathrm{eff}} \neq 3$ will be briefly discussed. For detailed formulas we refer to Refs. [14] and [15]. We will take $q^2 = m_b^2/2$ [16] in penguin coefficients to generate favorable absorptive parts via short distance rescattering. Smaller q^2 values would lead to much smaller a_{CP}s. Thus, the CP asymmetries that we present are for sake of showing the trend only. As an indication of possible sensitivity to factorization scale μ_f, we list a_i^{eff} for $\mu_f = m_b$ and $m_b/2$ in Table I.

As we are interested in studying γ dependence of decay amplitudes, it is important to check the γ dependence of short distance coefficients. Although the a_i's for $b \rightarrow s$ penguins are basically γ-independent because $V_{us}^* V_{ub}$ is much smaller than $V_{ts}^* V_{tb} \simeq -V_{cs}^* V_{cb}$, it is not the case for $b \rightarrow d$ penguin coefficients since all three KM factors are on the same footing in $V_{ud}^* V_{ub} + V_{cd}^* V_{cb} + V_{td}^* V_{tb} = 0$. Thus, for $b \rightarrow d$ penguin coefficients, a_{3-10} will also exhibit γ dependence. In Fig. 1 we show the γ dependence of a_4, a_6, and a_9 for both $b \rightarrow d\bar{q}q$ and $\bar{b} \rightarrow \bar{d}\bar{q}q$. These are the dominant gluonic and electroweak penguin coefficients. We see that for $\gamma = 50° - 150°$, $\mathrm{Re}\,a_4$ and $\mathrm{Re}\,a_6$ are within 3% of -0.0383 and -0.0437, respectively, while $\mathrm{Re}\,a_9$ is constant. These values are basically the same as $b \rightarrow s$ penguin coefficients. Variations of $\mathrm{Im}(a_{4,6})$ are more sizable but they are less significant than $\mathrm{Re}(a_{4,6})$ in contributing to average rates. Thus, given the present experimental uncertainties as well as underlying uncertainties associated with the factorization assumption, to first approximation the γ-dependence of $b \rightarrow d$ penguin coefficients can be safely ignored. In the following numeric results, however, γ-dep. of $b \rightarrow d$ penguin coefficients have been taken into account.

Let us see how tree-penguin interference gives us a bearing on $\cos\gamma$. Using the standard phase convention [9] of putting CP phase in $V_{ub} = |V_{ub}|e^{-i\gamma}$, the tree amplitudes ($O_1$ and O_2) for $b \rightarrow u\bar{u}d$ and $b \rightarrow u\bar{u}s$ processes have the KM factors

$$V_{ud}^* V_{ub} \cong |V_{ub}|e^{-i\gamma} \quad \text{and} \quad V_{us}^* V_{ub} \cong \lambda|V_{ub}|e^{-i\gamma},$$
$$(2.4)$$

respectively, where $\lambda \equiv |V_{us}| \cong 0.22$. The penguin amplitudes (O_{3-10}), on the other hand, are governed by the KM factors

TABLE I. Values for a_i^{eff} for $b \rightarrow s\bar{q}q$ processes for $N_c = 3$, evaluated at $\mu_f = m_b$ (first row) and $m_b/2$, where μ_f is the "factorization scale" (a_{3-10}^{eff} are in units of 10^{-4}). We take $q^2 = m_b^2/2$ in determining the imaginary parts.

a_1	a_2	a_3	a_4	a_5	a_6	a_7	a_8	a_9	a_{10}
1.046	$+0.024$	72	$-383-121i$	-27	$-435-121i$	$-0.9-2.7i$	$3.3-0.9i$	$-93.9-2.7i$	$0.3-0.9i$
1.059	-0.048	96	$-396-120i$	-54	$-514-120i$	$-0.5-2.7i$	$4.0-0.9i$	$-93.2-2.7i$	$3.6-0.9i$

TABLE II. Form factors at zero momentum transfer in the BSW model [12] and in the LC sum rule calculations [11]. The values given in the square brackets are obtained in the LC sum rule analysis.

Decay	$F_1 = F_0$	V	A_1	A_2	A_0
$B \to \pi$	0.333 [0.305]				
$B \to K$	0.379 [0.341]				
$B \to \rho$		0.329 [0.338]	0.283 [0.261]	0.283 [0.223]	0.281 [0.372]
$B \to K^*$		0.369 [0.458]	0.328 [0.337]	0.331 [0.203]	0.321 [0.470]

$$V_{td}^* V_{tb} = -(V_{cd}^* V_{cb} + V_{ud}^* V_{ub}) \cong + (\lambda |V_{cb}| - |V_{ub}| e^{-i\gamma}), \quad (2.5)$$

$$V_{ts}^* V_{tb} = -(V_{cs}^* V_{cb} + V_{us}^* V_{ub}) \cong - (|V_{cb}| + \lambda |V_{ub}| e^{-i\gamma})$$

$$\cong - |V_{cb}|, \quad (2.6)$$

where KM unitarity, implicit in Eq. (2.1), has been used, and the last step for $V_{ts}^* V_{tb} \cong -|V_{cb}|$ is accurate to less than 2%. Since $|V_{ub}/V_{cb}| \approx 0.08$, one finds $\lambda - |V_{ub}/V_{cb}| \cos \gamma > 0$ always hence the real parts of $V_{td}^* V_{tb}$ and $V_{ts}^* V_{tb}$ are opposite in sign. Thus, *not only T-P interference for $b \to u\bar{u}d$ and $b \to u\bar{u}s$ processes depend on the sign of $\cos \gamma$, the interference effect is opposite between the two type of processes*, e.g. when constructive in $K^+ \pi^{-,0}$ for $\cos \gamma < 0$, it is destructive in $\pi^+ \pi^-$, which is precisely what is needed to explain data.

Such phenomena are of fundamental nature, and offer a window on the phase angle γ, but it can be obscured by long distance effects such as $\pi^+ \pi^- \to \pi^0 \pi^0$ [7,14] rescattering. However, the nonobservation of $B \to K\bar{K}$ mode indicates that inelastic rescattering is not sizable, while absence of $\pi^0 \pi^0$ mode suggests that the smallness of $\pi^+ \pi^-$ is not due to $\pi^+ \pi^- \to \pi^0 \pi^0$ rescattering [see Note added]. As discussed in Ref. [5] for $K\pi$ modes, a rescattering phase of 60° or more is needed before appreciable deviations from our results would set in. The only exception against factorization is $B^+ \to K^+ \omega^0 \sim 1.5 \times 10^{-5}$ [2], which we can only wait for experimental confirmation [see Note added]. In the mean time, we note that factorizaton is more likely to work in the N_C insensitive modes such as the ones studied here. That is, a 20–30 % change in $1/N_C$ should have little impact. We note in passing that some recent work in applications of perturbative QCD to B decays are beginning to reveal how factorization works [17].

III. COMPARISON OF $B \to PP$, PV MODES WITH DATA

It was $B \to PP$, PV data that *inspired* the observation that factorization does work and hinted at $\cos \gamma < 0$ in Nature. The starting point was the $K\pi$ modes. Ignoring the electroweak penguin (EWP) amplitude, one typically expects $K^+ \pi^0 / K^+ \pi^- \approx (1/\sqrt{2})^2$, where the factor of $1/\sqrt{2}$ comes from the π^0 isospin wave function, and the ratio is almost independent of γ. The data, however, suggest that $K^+ \pi^0$ is as large as $K^+ \pi^-$ [1,3], which imply that EWP may be important [5,6]. Choosing larger m_s to suppress strong penguin a_6 contribution, and γ *in the range of* 90° − 130° *to enhance* $K^+ \pi^-$ *and* $K^+ \pi^0$ with respect to $K^0 \pi^+$, it was

shown [5] that the three observed $K\pi$ modes can be suitably close to each other and the data are thus accommodated [see Note added].

The $\pi^+ \pi^-$ mode then presents a challenge. It is color allowed and should be T-dominant, and easier to see experimentally than the recently measured $B^+ \to \rho^0 \pi^+$ and $B^0 \to \rho^\pm \pi^\mp$ modes [3]. However, it is not yet observed [see Note added]. Without resorting to a small $N_{\text{eff}} \sim 1$ or large final state rescattering phases, it was pointed out that suppression of the $\pi^+ \pi^-$ mode can be elegantly achieved if $\cos \gamma < 0$, which would enhance the $\rho^0 \pi^+$ mode (and even more so if $m_u + m_d$ is on the lighter side) and suppress $\rho^\pm \pi^\mp$ [7]. If the $A_0^{B \to \rho}(q^2 = m_\pi^2)$ form factor is larger than in BSW model [12], it could further help explain the strength of $\rho^0 \pi^+ \sim 1.5 \times 10^{-5}$ and the smallness of the ratio $\rho^\pm \pi^\mp / \rho^0 \pi^+ = 2.3 \pm 1.3$ [3].

The newly measured $K^{*+} \pi^-$ mode is also color allowed and insensitive to N_{eff}, while the $F_1^{B \to \pi}(m_{K*}^2)$ form factor is constrained by $B \to K\pi$, $K^+ \phi^0$, $\pi\pi$ and the semileptonic $B \to \pi(\rho) l \nu$ data. The factorization approach gives too low a value of $K^{*+} \pi^- < 0.7 \times 10^{-5}$ [7] for $\gamma \sim 60° - 70°$. Choosing a larger γ such as $\sim 120°$, however, $K^{*+} \pi^-$ can easily reach 1.2×10^{-5} or more [7] and becomes more consistent with data.

The above observations are largely insensitive to N_{eff}. In Ref. [7] BSW form factors were used. In fact, the form factors from light-cone sum rules [11] seem to give a better fit to $B \to PP$, PV data, since the A_0 form factor is larger while $F_{0,1}$ form factors are slightly lower than in BSW model. We list the relevant form factor values at zero momentum transfer for both BSW model and LC sum rules in Table II. The q^2 dependence of the LC sum rule results can be referred to [11]. Note that hadronic charmless $B \to PP$ and VP are insensitive to the q^2 dependence of form factors because of the smallness of q^2 in the factorization approach. However, if $F_1^{B \to P}(q^2)$ has dipole q^2 dependence, the $K^{*+} \pi^-$ rate can be enhanced by 12% because $q^2 = m_{K*}^2$ is no longer negligible.

At this point we caution that form factor models typically do not have good reference to the factorization scale μ_f that enters a_i^{eff}. Thus, until one has a more complete model of how factorization works, one should bear in mind the uncertainties in a_i^{eff} that may follow from changing $\mu_f = m_b$ to $m_b/2$, as reflected in Table I. In the complete theory, there should again be no μ_f dependence. We note that some progress has been made recently in providing a QCD basis for why and how factorization works [17].
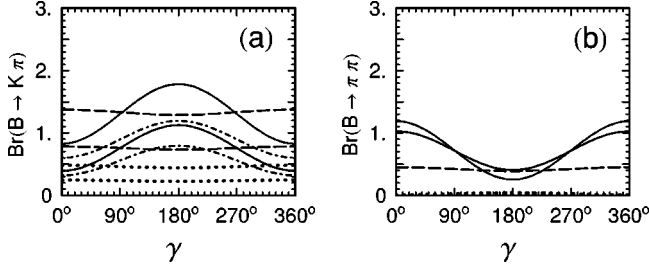
FIG. 2. (a) Solid, dash, dotdash and dots for $B \to K^+\pi^-$, $K^0\pi^+$, $K^+\pi^0$ and $K^0\pi^0$, for $m_s = 105$ (upper curves) and 200 MeV; (b) solid, dash and dots for $B \to \pi^+\pi^-$, $\pi^+\pi^0$ and $\pi^0\pi^0$ for $m_d = 2m_u = 3$ and 6.4 MeV, where the lower (upper) curves at $\gamma = 180°$ for $\pi^+\pi^-$ ($\pi^0\pi^0$) are for lower $m_u + m_d$. In all figures $|V_{ub}/V_{cb}| = 0.08$, Brs are in units of 10^{-5}, and light cone sum rule form factors are used.

The results using BSW form factors have been given in [7]. Here, for comparison we use LC sum rule (LCSR) form factors and plot the results versus γ in Figs. 2, 3 and 4. The $K\pi$ and $\pi\pi$ modes fit data rather well, except $K^+\pi^- > K^+\pi^0$ is expected [see Note added] if one picks $m_s \sim 100$ MeV. As emphasized in [7], a larger value of $A_0^{B\rho}$ (which is realized in the LCSR approach), would pull up the $\rho^0\pi^+$ and $\omega^0\pi^+$ rates. Having $\rho^0\pi^+ > \omega^0\pi^+$ which is hinted by data would still prefer $\gamma \gtrsim 90°$. Because of a lower F_1^{BK}, the Br of $\phi^0 K^+$ drops to 0.5×10^{-5}, which again fits better the experimental upper limit of 0.59×10^{-5} [3]. The $\rho^\pm\pi^\mp$ rate is now lower because $B^0 \to \rho^+\pi^-$ amplitude depends on $F_1^{B\pi}$ only, while $B^0 \to \rho^-\pi^+$ is enhanced by a larger $A_0^{B\rho}$ analogous to $\rho^0\pi^+$. For $\gamma = 120° - 150°$ and lighter $m_d + m_u$, $\rho^\pm\pi^\mp \sim 3 \times 10^{-5}$ and $\rho^0\pi^+$, $K^{*+}\pi^- \sim 1 \times 10^{-5}$. These values are lower than but within range of recent CLEO observations [3].

Because the form factors from LC sum rule calculations fit data better, we adopt the LCSR form factors in subsequent analysis of further modes. We stress that this is only for numerical expedience. One should not take LC sum rule form factors as more secure since it is based just on another dynamical computation.
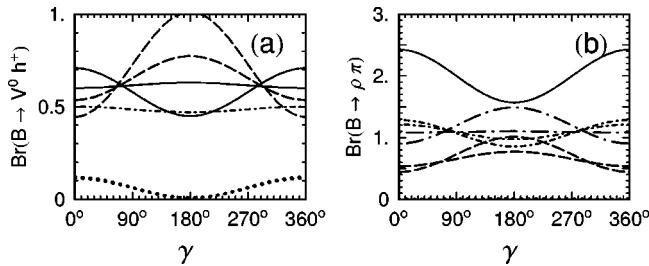

FIG. 3. For $m_d = 2m_u = 3$ and 6.4 MeV, (a) solid, dash, dotdash and dots for $\omega^0\pi^+$, $\rho^0\pi^+$, $\phi^0 K^+$ and $\omega^0 K^+$; (b) solid, short-dotdash, long-dotdash, dash and dots for $B \to \rho^+\pi^-$, $\rho^+\pi^0$, $\rho^-\pi^+$, $\rho^0\pi^+$ and $\rho^0\pi^0$. The upper curves at $\gamma = 180°$ are for lower m_d and m_u.

IV. ANALYSIS OF γ-DEPENDENCE OF FURTHER MODES

A. $B \to \rho\rho$ and $\rho\omega$ modes

$B \to VV$ amplitudes are independent of light quark masses. The modes $\rho^+\rho^-$, $\rho^+\rho^0$, and $\rho^+\omega^0$ are all of order 10^{-5} with $\rho^+\rho^-$ being the largest. One expects $\rho^+\rho^-/\rho^+\omega^0 \approx (1/\sqrt{2})^2$ where $1/\sqrt{2}$ comes from the ω^0 isospin wave function. The γ-dependence of $\rho^+\rho^-$ and $\rho^+\omega^0$ rates is dominated by the interference term $\propto \mathrm{Re}(V_{ud}^* V_{ub} a_1) \times \mathrm{Re}(V_{td}^* V_{tb} a_4)$. In contrast, the $\rho^+\rho^0$ mode is far less sensitive to γ since a_4 is replaced by $3a_9/2$ where a_9 is ~ 4 times smaller than a_4. In any case, all three modes get suppressed for $\cos\gamma < 0$, as shown in Fig. 5. For the currently favored value of $\gamma \sim 60° - 70°$ [8], one expects $\rho^+\rho^-:\rho^+\rho^0:\rho^+\omega^0 \approx 3.1:1.7:1.7$ (roughly $\times 10^{-5}$), but if γ is larger than $90°$, say $\sim 120°$, it becomes $2.5:1.6:1.2$, reaching down to $2.3:1.5:1.0$ at $\gamma \sim 180°$. Thus, finding $\rho^+\omega^0 < \rho^+\rho^0$ would support $\cos\gamma < 0$, similar to $\omega^0\pi^+ < \rho^0\pi^+$. The branching ratios imply that these modes could be observed soon. However, $\rho^+\rho^- \to \pi^+\pi^0\pi^-\pi^0$ has two π^0's in the final state and would be harder to detect than the other two modes, while $\rho^+\omega^0$ is expected to have the least background.

To study model dependence, we have also used form factor values from BSW model [12] as input parameters. We find that the ratios do not change much, but the overall scale can become smaller by 40%.

The a_{CP}s are dominated by $\mathrm{Im}(V_{ud}^* V_{ub}) a_1 \mathrm{Re}(V_{td}^* V_{tb})$ times $\mathrm{Im}(a_4)$, $2\,\mathrm{Im}(a_4)$ and $\mathrm{Im}(3a_9/2)$ terms for $\rho^+\rho^-$, $\rho^+\omega^0$ and $\rho^+\rho^0$, respectively. As seen from Fig. 5, the a_{CP}s for $\rho^+\rho^-$, $\rho^+\omega^0$ could be as large as -7%, -16%, respectively, for $\gamma = 90° - 130°$, while for $\rho^+\rho^0$ it is very small since the strong P contribution is forbidden by isospin. The a_{CP}s are smaller for $\gamma \sim 60° - 70°$.

B. $B \to K^*\rho$ modes and the electroweak penguin amplitude

Tree-penguin interference for $K^{*+}\rho$ and $\rho^+\rho$ modes differ in sign because the KM factors $\mathrm{Re}(V_{td}^* V_{tb}) \cong A\lambda^3(1-\rho)$ and $\mathrm{Re}(V_{ts}^* V_{tb}) \cong -A\lambda^2$ have opposite sign, quite analogous to the case of $K^+\pi^{-,0}$ vs $\pi^+\pi^-$ [7]. Thus, while $\rho^+\rho^-$ and $\rho^+\omega^0$ are suppressed for $\cos\gamma < 0$, $K^{*+}\rho$ modes are enhanced. Furthermore, the impact of EWP on $K^*\rho^0$ modes is more prominent than on the $K\pi^0$ [5] and $K^*\pi^0$ [7] modes which have similar amplitude structure.

Let us show how the latter comes about. For $K^+\pi^0/K^+\pi^-$, we have

$$\frac{K^+\pi^0}{K^+\pi^-} \approx \frac{1}{2}\left| 1 + r_0 \frac{\lambda\left|\dfrac{V_{ub}}{V_{cb}}\right| e^{-i\gamma} a_2 + \dfrac{3}{2} a_9}{\lambda\left|\dfrac{V_{ub}}{V_{cb}}\right| e^{-i\gamma} a_1 + a_4 + a_6 R_4} \right|^2$$

$$\approx \begin{cases} 0.65, & m_s = 105 \text{ MeV} \\ \mathcal{O}(1), & m_s \text{ large,} \end{cases} \qquad (4.1)$$

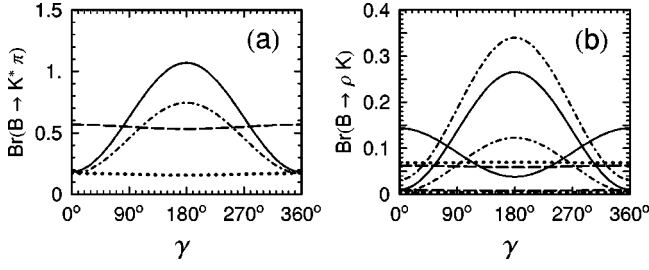where the factor of $1/2$ is from the π^0 isospin wave function,

FIG. 4. (a) Solid, dash, dotdash and dots for $B \to K^{*+}\pi^-$, $K^{*0}\pi^+$, $K^{*+}\pi^0$ and $K^{*0}\pi^0$, which are insensitive to m_s. (b) Solid, dash, dotdash and dots for $\rho^- K^+$, $\rho^+ K^0$, $\rho^0 K^+$ and $\rho^0 K^0$, for $m_s = 105$ and 200 MeV. The upper (lower) curves for ρK^0 (ρK^+) at $\gamma = 180°$ are for lower m_s.

$r_0 = f_\pi F_0^{BK}/f_K F_0^{B\pi} \simeq 0.9$ in both LCSR and BSW models, and light quark masses enter through $R_4 = 2m_{K'}^2/(m_b - m_u)(m_s + m_u)$. Although at present [1] $K^+\pi^0/K^+\pi^- \approx 1$ seems to favor [5] large m_s to suppress the penguin a_6 term, for more sensible $m_s < 200$ MeV values, $K^+\pi^0$ is always visibly less than $K^+\pi^-$ [7], as can be seen in Fig. 2(a).

For $K^{*+}\pi^0/K^{*+}\pi^-$, the a_6 term is absent, but the a_2 and EWP a_9 terms are modulated by the factor $r_1 = f_\pi A_0^{BK^*}/f_{K^*} F_1^{B\pi} = 0.9$ (0.6) in LCSR (BSW) model, and

$$\frac{K^{*+}\pi^0}{K^{*+}\pi^-} \approx \frac{1}{2}\left| 1 + r_1 \frac{\lambda\left|\frac{V_{ub}}{V_{cb}}\right| e^{-i\gamma}a_2 + \frac{3}{2}a_9}{\lambda\left|\frac{V_{ub}}{V_{cb}}\right| e^{-i\gamma}a_1 + a_4} \right|^2$$

$$\approx 0.7 \quad (0.6) \quad \text{in LCSR (BSW)}, \qquad (4.2)$$

as can be seen from Fig. 4(a).

For $K^{*+}\rho^0/K^{*+}\rho^-$, r_1 is replaced by a more complicated ratio of ρ and K^* decay constants and $B \to V$ form factors, and

$$\frac{K^{*+}\rho^0}{K^{*+}\rho^-} \approx \frac{1}{2}\left| 1 + r_2 \frac{\lambda\left|\frac{V_{ub}}{V_{cb}}\right| e^{-i\gamma}a_2 + \frac{3}{2}a_9}{\lambda\left|\frac{V_{ub}}{V_{cb}}\right| e^{-i\gamma}a_1 + a_4} \right|^2 \approx 1, \quad (4.3)$$

since $r_2 \simeq 1.2$ ($\simeq 1.1$ for BSW form factors) turns out to be larger than r_1. Again, absolute rates are sensitive to form factor models, but ratios in general are not.
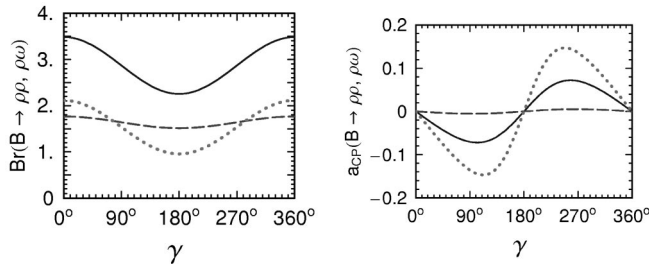

FIG. 5. Brs and a_{CP}s vs γ where solid, dash and dots are for $\rho^+\rho^-$, $\rho^+\rho^0$ and $\rho^+\omega^0$, respectively.
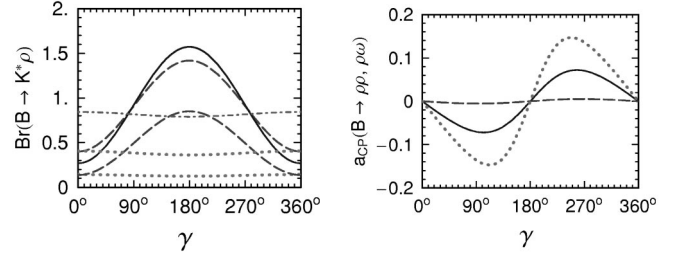
FIG. 6. Brs and a_{CP}s vs γ where solid, dash, dotdash and dots are for $K^{*+}\rho^-$, $K^{*+}\rho^0$, $K^{*0}\rho^+$ and $K^{*0}\rho^0$, respectively. Setting the EWP term $a_9 = 0$ lowers (raises) the $K^{*+}\rho^0$ ($K^{*0}\rho^0$) rate, while the upper a_{CP} curve for $K^{*+}\rho^0$ becomes very close to the $K^{*+}\rho^-$ case.

Thus, *the EWP effect is most prominent in the $K^*\rho^0$ modes*, which enhances the ratio $K^{*+}\rho^0/K^{*+}\rho^-$ to be close to 1. It also suppresses the $K^{*0}\rho^0$ mode. To illustrate this we show in Fig. 6 both the cases of keeping a_9 and with a_9 set to 0. Thus, we see that *the EWP effect is able to enhance the $K^{*+}\rho^0$ rate by a factor of 2!* In comparison, the EWP effect in $K^+\pi^0$ is diluted by the additional strong penguin contribution from a_6, while for $K^{*+}\pi^0/K^{*+}\pi^-$, it is subdued by the form factor ratio r_1. If r_1 is even larger than LCSR case, then $K^{*+}\pi^0/K^{*+}\pi^-$ could be closer to 1. We note that the rate difference between $K^*\rho^0$ and $K^*\omega^0$ (which we discuss below) modes is also mainly due to the EWP contribution.

We find that, for $\gamma \sim 60° - 70°$ one has $K^{*0}\rho^+ \gtrsim K^{*+}\rho^0 \approx K^{*+}\rho^- \gg K^{*0}\rho^0$, but for $\cos\gamma < 0$ it becomes $K^{*+}\rho^- \gtrsim K^{*+}\rho^0 > K^{*0}\rho^+ \gg K^{*0}\rho^0$. The a_{CP}s of $K^{*+}\rho^-$ and $K^{*+}\rho^0$ modes are sizable and have opposite sign to $\rho^+\rho^-$ and $\rho^+\omega^0$ modes. For $\gamma \sim 65°$ they could be as large as 30% and 18% respectively, but are of order 15% or 10% for $\gamma \sim 120°$.

C. $B \to K^*\omega$ and $K^*\phi$ modes

The sign of $T-P$ interference in $K^{*+}\omega^0$ and $K^{*+}\rho^0$ modes are rather similar under factorization. Thus, the $K^{*+}\omega^0$ rates are also enhanced in the region of $\cos\gamma < 0$, as can be seen in Fig. 7. The $K^{*0}\omega^0$ rate is insensitive to γ because its tree contribution is color suppressed. Thus, the $K^{*+}\omega^0$ rate can be 1.5–2.5 times larger than $K^{*0}\omega^0$ for $\cos\gamma < 0$, while $K^{*+}\omega^0 \lesssim K^{*0}\omega^0$ for $\gamma \sim 60° - 70°$. Since T/P is of order 20–30 %, direct a_{CP} for $K^{*+}\omega^0$ could reach 40% for $\gamma \sim 60° - 70°$, and could still be 20% even for $\gamma \sim 120°$.

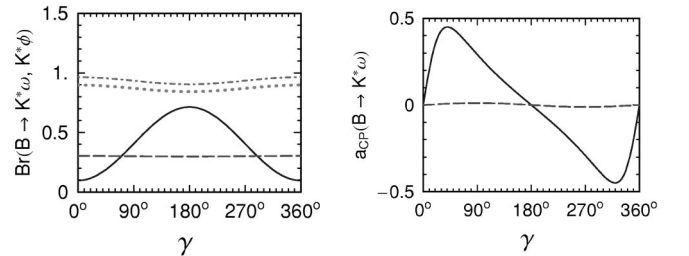FIG. 7. Brs and a_{CP}s vs γ where solid, dash, dotdash and dots are for $K^{*+}\omega^0$, $K^{*0}\omega^0$, $K^{*+}\phi^0$ and $K^{*0}\phi^0$, respectively. The a_{CP}s of $K^*\phi$, not shown here, are consistent with zero.
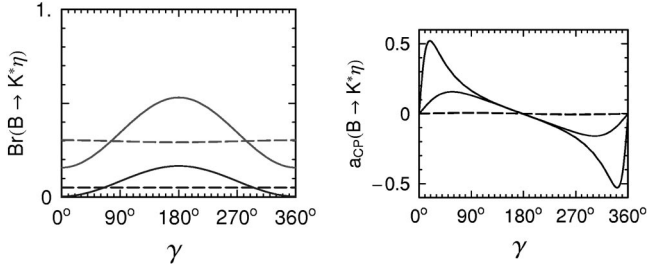
FIG. 8. Brs and a_{CP}s vs γ where solid and dash are for $K^{*+}\eta$ and $K^{*0}\eta$, respectively, for $m_s = 105$ and 200 MeV. Upper curves for Brs are for $m_s = 105$ MeV while for a_{CP}s the sharper curve is for $m_s = 200$ MeV.

FIG. 9. Brs vs γ where (a) solid, dash, dotdash and dots are for $K^+\eta$, $K^0\eta$, $K^{*+}\eta'$ and $K^{*0}\eta'$, respectively; (b) solid and dash are for $K^0\omega^0$ and $K^+\omega^0$, respectively. The upper (lower) curves for $K\eta$ and $K^0\omega^0$ at $\gamma = 180°$ are for $m_s = 105$ (200) MeV, while for $K^*\eta'$ and $K^+\omega^0$ it is the reverse.

The $K^*\phi^0$ modes arise from the pure penguin $b \to s\bar{s}s$ process and have very weak γ dependence (Fig. 7). Though not useful for extracting γ, they give a more direct test of the factorization hypothesis. In the standard model the a_{CP}s are practically zero and any measurement $\geq 10\%$ would likely be an indication for new physics [18].

D. $B \to K^*\eta$ modes

As pointed out in Ref. [7], having $\cos\gamma < 0$ could explain the observed splitting of $K^+\eta' > K^0\eta'$, although the $K\eta'$ modes seem to have a large singlet contribution, such as coming from the anomaly [19]. Even assuming $N_{\text{eff}}(LL) = 2 \neq N_{\text{eff}}(LR) = 5$ [14] and low m_s values, the rates fall 30–40 % short of observed, while for $N_{\text{eff}} = 3$ one can only account for less than half the observed rate. Since we do not know how to take the anomaly effect into proper account for exclusive modes, we shall not plot the results here.

The $K^*\eta$ modes, however, should be less susceptible to the anomaly effect, and with T/P structure similar to $K^*\pi^0$ [7]. Ignoring the extra anomaly term and omitting an overall factor of $\sqrt{2}G_F m_{K^*}\epsilon_{K^*} \cdot p_B$, one has

$$\mathcal{M}_{K^{*0}\eta^{(')}} \cong V^*_{us}V_{ub}f^u_{\eta^{(')}}A_0 a_2 - V^*_{ts}V_{tb}\Bigg[(f_{K^*}F_1 + f^s_{\eta^{(')}}A_0)a_4$$

$$- (f^u_{\eta^{(')}} - f^s_{\eta^{(')}})A_0\Bigg(a_6 Q^{(')} - \frac{1}{2}a_9\Bigg)\Bigg],$$

$$\mathcal{M}_{K^{*+}\eta^{(')}} \cong \mathcal{M}_{K^{*0}\eta^{(')}} + V^*_{us}V_{ub}f_{K^*}F_1 a_1, \qquad (4.4)$$

where $Q^{(')} = -m^2_{\eta^{(')}}/(m_b + m_s)m_s$, $F_1 = F^{B\eta^{(')}}_1(m^2_{K^*})$, $A_0 = A^{BK^*}_0(m^2_{\eta^{(')}})$ and we have dropped terms that are much smaller than those shown. Numerically we use f^u_η, $f^s_\eta = 78$, -112 MeV, and $f^u_{\eta'}$, $f^s_{\eta'} = 63$, 137 MeV [14]. The γ dependence for $K^{*0}\eta$ mode is weak because the tree contribution is color suppressed. For $K^{*+}\eta$ one has constructive T–P interference for $\cos\gamma < 0$ hence $K^{*+}\eta > K^{*0}\eta$ while $K^{*+}\eta \lesssim K^{*0}\eta$ for $\gamma \sim 60°$–$70°$. As shown in Fig. 8, the rates depend strongly on m_s, the strange quark mass. We find $K^{*+}\eta/K^{*0}\eta \approx 1.5$ for $m_s = 105$ MeV, but may be enhanced to 2.2 for $m_s = 200$ MeV. The rates could be larger
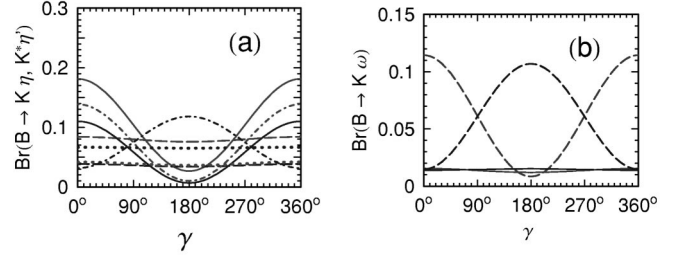
by 50% or more since A^{BV}_0 seems to be larger [7] than F^{BP}_1, as indicated by the strength of the $\rho^0\pi^+$ mode.

E. Various suppressed modes

The $\rho^0\rho^0$, $\rho^0\omega^0$, and $\omega^0\omega^0$ modes are color suppressed and dominated by penguin contributions which have opposite sign compared to $\rho^+\rho^{-,0}$ and $\rho^+\omega^0$ case. The rates are enhanced for $\cos\gamma < 0$ but are, however, only of order 10^{-7}. The $\rho^0\phi^0$, $\rho^+\phi^0$ and $\omega^0\phi^0$ modes are pure penguin processes with amplitudes $\propto V^*_{td}V_{tb}[a_3 + a_5 - (a_7 + a_9)/2]$. Their rates are too small ($\sim 10^{-8}$) to be measurable soon, and their a_{CP}s are practically zero.

The $K^*\eta'$ modes are suppressed because $f^s_{\eta'} > 0$, as can be seen from Eq. (4.4). Likewise, $K\eta$ modes are also suppressed. The Brs are given in Fig. 9. We see that $K^*\eta' \lesssim 1.5 \times 10^{-6}$, and for $\cos\gamma < 0$ the $K^+\eta$ rate is suppressed, leading to $K^+\eta \lesssim K^0\eta \lesssim 10^{-6}$. These suppressed modes should be compared with the $K\eta'$ modes, which are already observed and are the largest exclusive rare hadronic decays, and the $K^*\eta$ modes, which have some chance of being observed in the near future.

The $K^+\omega^0$ mode is reported at the rather sizable level of 1.5×10^{-5} [2], in strong conflict with the rather suppressed factorization expectation [see Note added]. This is also illustrated in Fig. 9 together with $K^0\omega^0$, which has lower reconstruction efficiency. The $K\omega^0$ rates are also very sensitive to m_s, but we do not see any way to enhance them within factorization approach.

In general, when modes are suppressed because of cancellation of different contributions such as the modes shown in Fig. 9, one is not only sensitive to form factors and long distance effects, but also sensitive to actual values of short distance coefficients.

V. DISCUSSION AND CONCLUSION

The $B \to VV$ decay rates are quite sensitive to the chosen form factor model, but the relative sizes of Brs and a_{CP}s are not. We find that BSW model form factors lead to 40% or so smaller Brs compared to using LC sum rule form factors. But all Brs could easily be larger than shown here by 50% or more if $B \to V$ form factors are in general larger [7] than $B \to P$ form factors, as indicated by the strength of the $\rho^0\pi^+$

mode [3]. We of course have not exhausted variations in form factor models. Furthermore, the need for form factor models arises under factorization. A more fundamental approach for calculating hadronic matrix elements should in principle bypass the issue of form factors. Our main results are insensitive to $N_{\text{eff}} \neq 3$. For $N_{\text{eff}} < 3$, the $\rho^+\rho^0$ and $\rho^+\omega^0$ modes are enhanced and become closer to $\rho^+\rho^-$. For $N_{\text{eff}} = 2$, the $\rho^0\rho^0$ and $\omega^0\omega^0$ modes become one order of magnitude larger, but still below 10^{-6}.

Subsequent to Ref. [7], the observation of $\rho^\pm\pi^\mp$ and $K^{*+}\pi^-$ modes [3] were reported, which offer further support for the factorization and $\cos\gamma < 0$ hypotheses. We believe that the $\pi^+\pi^-$, $\pi^+\pi^0$, $\rho^+\pi^0$, $\omega^0\pi^+$, $K^{*+}\pi^0$ and $K^{*0}\pi^+$ modes, all discussed in Ref. [7], would likely emerge with full CLEO II and II.V datasets [see *Note added*]. The $K^{(*)0}\pi^0$ modes are borderline, the ρK modes unlikely, while $\pi^0\pi^0$ and $\rho^0\pi^0$ modes should not be seen soon if factorization is correct. But what are the modes discussed here that are promising for detection in the near future? As mentioned in Ref. [7], the theoretical computation of VV and $\eta^{(\prime)}$ modes are less trustworthy even under factorization assumption, as they depend on vector form factors or $\eta^{(\prime)}$ decay constants. We give a discussion nevertheless.

Since helicity angle methods (boosted π^+, K^+ or π^0 along parent $\rho^{+,0}$ or $K^{*+,0}$ momentum) seem promising from observed $\rho^\pm\pi^\mp$ reconstruction [3], the modes $K^{*+}\rho^0$ and $\rho^+\rho^0$ with $\rho^0 \to \pi^+\pi^-$ can probably be reconstructed above background. It is less clear whether this is the case for $\rho^+\rho^-$ and $K^{*+}\rho^-$. The $K^{*0}\rho^+$ mode is at best borderline even without considering background, while $K^{*0}\rho^0 \sim 10^{-6}$ is unlikely to be observed soon.

The reconstruction of two body modes containing an ω^0 has been shown [2] to be of low background and with efficiency better than η' modes. Assuming that the $B \to V$ form factors $A_{1,2}$ and V are similarly enhanced as A_0, the $\rho^+\omega^0$ and perhaps the $K^{*+}\omega^0$ modes could be observed soon, while $K^{*0}\omega^0$ is at best borderline. The four $K^{(*)}\phi^0$ modes should also suffer little from background. The $K^*\phi^0$ modes could be split above $K\phi^0$ modes if $B \to K^*$ form factors are enhanced over $B \to K$. At the 0.5×10^{-5} level, the $K^+\phi^0$ and $K^{*+}\phi^0$ modes are likely to appear soon, while $K^0\phi^0$ and $K^{*0}\phi^0$ modes suffer from detection efficiency and may be borderline. The $K^{*+}\eta$ mode could emerge if $A_0^{BK^*}$ is large, but $K^{*0}\eta$ is probably borderline. These modes should again have low background.

All the suppressed modes mentioned in Sec. IV E should not appear. The nonobservation of $K\bar{K}$ modes so far suggest inelastic final state rescattering effects are small. However, the observation of $K\omega$, $K\rho$ or any of the suppressed modes under factorization may indicate the size of final state rescat-

tering, hence the level of breakdown of factorization. We cannot account for the observed large $K^+\omega^0 \sim 1.5 \times 10^{-5}$ in factorization approach, and await further updates with full CLEO II and II.V datasets [see Note added].

In conclusion, we have studied the γ dependence of hadronic rare B decays to PP, PV, VV and $K^*\eta$ modes within the factorization approach. We find that light cone sum rule form factors give better fit to $B \to PP$, PV data. The $\rho^+\omega^0$, $\rho^+\rho^0$, $K^{*+}\rho^0$ and $K^{(*)+}\phi^0$, and perhaps the $K^{*+}\omega^0$ and $K^{*+}\eta$ modes, should be observable with the full CLEO II and II.V datasets. Whether the sizable $\rho^+\rho^-$ and $K^{*+}\rho^-$ modes can be observed depends crucially on the background level, while the clean modes of $K^{(*)0}\phi^0$ are probably borderline because of statistics. The $K^{*0}\rho^0$, $K^{*0}\omega^0$ and $K^{*0}\eta$ modes are likely too low to be seen with 10^7 $B\bar{B}$s. Finding $\rho^+\omega^0 < \rho^+\rho^0$, $K^{*+}\rho^{-,0} > K^{*0}\rho^+$, $K^{*+}\omega^0 > K^{*0}\omega^0$ and $K^{*+}\eta > K^{*0}\eta$ would support $\cos\gamma < 0$. The EWP effect should be most prominent in $K^{*+}\rho^0$ mode as compared to $K^{(*)+}\pi^0$, leading to a factor of two enhancement in rate, and observation of $K^{*+}\rho^0 \simeq K^{*+}\rho^-$ would give strong evidence for the electroweak penguin amplitude. The weakly γ-dependent pure penguin processes $K^{(*)}\phi^0$ can be used as a direct test of the factorization hypothesis. If large a_{CP} is measured in $K^{(*)+}\phi^0$ modes, then new physics would be implied.

The rare $B \to VV$ modes should also be studied with vigor.

Note added. Upon completion of this paper, CLEO announced [20] new results at the summer conferences. The long sought-after $\pi^+\pi^-$ mode is found at $(0.47^{+0.18}_{-0.15} \pm 0.13) \times 10^{-5}$. The ωK^+ mode has disappeared under the 90% upper limit of $< 0.8 \times 10^{-5}$, in strong contrast to the published value of $(1.5^{+0.7}_{-0.6} \pm 0.2) \times 10^{-5}$ [2]. At the same time, the previously unmeasured $\omega\pi^+$ mode is now measured at $(1.1 \pm 0.3 \pm 0.1) \times 10^{-5}$. The $K^+\pi^-$ mode is also updated to $(1.88^{+0.28}_{-0.26} \pm 0.06) \times 10^{-5}$ and now larger than $K^+\pi^0$, while the surprising strength of the $\bar{K}^0\pi^0$ mode suggest that m_s could be even lighter. All these new results are in better agreement with the discussions presented in this paper. There is no indication of breakdown of factorization in rare B decays so far, so long as one takes $\cos\gamma < 0$. We note that the rather small value for $\pi^+\pi^-$ mode, together with the strength of $\rho\pi$ modes, make other explanations such as a smaller $|V_{ub}|$ implausible.

ACKNOWLEDGMENTS

[1] J. Alexander, plenary talk at ICHEP98, 1998, Vancouver.

[2] CLEO Collaboration, T. Bergfeld *et al.*, Phys. Rev. Lett. **81**, 272 (1998).

[3] Y. S. Gao and F. Würthwein, hep-ex/9904008, based on CLEO

results presented at DPF99 (1999, Los Angeles, USA) and APS99 (1999, Atlanta, USA).

[4] R. Fleischer and T. Mannel, Phys. Rev. D **57**, 2752 (1998).

[5] N. G. Deshpande *et al.*, Phys. Rev. Lett. **82**, 2240 (1999).

[6] M. Neubert and J. Rosner, Phys. Lett. B **441**, 403 (1998); M. Neubert, J. High Energy Phys. **02**, 14 (1999).

[7] X. G. He, W. S. Hou, and K. C. Yang, Phys. Rev. Lett. **83**, 1100 (1999).

[8] F. Parodi, P. Roudeau, and A. Stocchi, hep-ph/9802289; S. Mele, Phys. Rev. D **59**, 113011 (1999).

[9] Particle Data Group, C. Caso *et al.*, Eur. Phys. J. C **3**, 1 (1998).

[10] B. Tseng and C. W. Chiang, hep-ph/9905338, also discuss *VV* modes that touch upon, but do not emphasize, the issue of sign of cos γ.

[11] P. Ball and V. M. Braun, Phys. Rev. D **58**, 094016 (1998); P. Ball, J. High Energy Phys. **09**, 005 (1998).

[12] M. Wirbel, B. Stech, and M. Bauer, Z. Phys. C **29**, 637 (1985).

[13] H. Y. Cheng, H. n. Li, and K. C. Yang, Phys. Rev. D **60**, 094005 (1999).

[14] Y. H. Chen *et al.*, Phys. Rev. D **60**, 094014 (1999). In Ref. [7] the c_is were taken from H. Y. Cheng and B. Tseng, *ibid.* **58**, 094005 (1998), which would lead to some percentage differences compared to using c_i^{eff}.

[15] A. Ali, G. Kramer, and C. D. Lü, Phys. Rev. D **58**, 094009 (1998).

[16] J.-M. Gérard and W. S. Hou, Phys. Rev. Lett. **62**, 855 (1989).

[17] C. H. V. Chang and H. n. Li, Phys. Rev. D **55**, 5577 (1997); Y. T. Yeh and H. n. Li, *ibid.* **56**, 1615 (1997); M. Beneke *et al.*, Phys. Rev. Lett. **83**, 1914 (1999).

[18] X. G. He, W. S. Hou, and K. C. Yang, Phys. Rev. Lett. **81**, 5738 (1998).

[19] W. S. Hou and B. Tseng, Phys. Rev. Lett. **80**, 434 (1998).

[20] D. Jaffe, talk at 8th International Symposium on Heavy Flavor Physics, 1999, Southampton, England; R. Poling, plenary talk at the 19th International Symposium on Lepton and Photon Interactions (LP99), 1999, Stanford, USA.